



Design of a Reduction-Resistant $\text{Ce}_{0.8}\text{Sm}_{0.2}\text{O}_{1.9}$ Electrolyte Through Growth of a Thin $\text{BaCe}_{1-x}\text{Sm}_x\text{O}_{3-\alpha}$ Layer over Electrolyte Surface

Daisuke Hirabayashi,^a Atsuko Tomita,^a Takashi Hibino,^{b,*} Masahiro Nagao,^b and Mitsuru Sano^b

^aNational Institute of Advanced Industrial Science and Technology, Nagoya 463-8560, Japan

^bGraduate School of Environmental Studies, Nagoya University, Nagoya 466-0804, Japan

A method that can block off electronic current through a samaria-doped ceria (SDC, $\text{Ce}_{0.8}\text{Sm}_{0.2}\text{O}_{1.9}$) electrolyte is proposed. A thin BaCeO_3 -based layer 12 μm thick was grown by a solid-state reaction of the electrolyte substrate and a BaO film deposited previously over the substrate surface at 1500°C. A homogeneous junction between the layer and the electrolyte was formed, thus allowing no delamination and cracking of the layer. Tolerance of this layer to CO_2 was high enough to suppress decomposition into BaCO_3 and CeO_2 . Open-circuit voltages of a hydrogen-air fuel cell with the coated SDC electrolyte were near 1 V or more in the range of 600–950°C. The resulting peak power density was higher than that of a fuel cell with an uncoated SDC electrolyte. © 2004 The Electrochemical Society. [DOI: 10.1149/1.1786231] All rights reserved.

Manuscript submitted February 12, 2004; revised manuscript received February 27, 2004. Available electronically September 7, 2004.

Conventional solid-oxide fuel cells (SOFCs) using yttria-stabilized zirconia (YSZ) as the electrolyte are operated in the range of 800–1000°C to achieve sufficient ionic conduction in the electrolyte.¹ This limits the selection of materials due to the chemical reactivity and stability of the fuel-cell components at high temperatures. Furthermore, carbon deposition becomes serious for the anode when hydrocarbons are used as fuels. Accordingly, considerable research efforts have been devoted recently to developing SOFCs capable of operating below 800°C using electrolytes with higher ionic conductivity than YSZ.^{2–7}

Samaria- or gadolinia-doped ceria have been investigated previously as highly oxide-ion conducting electrolytes.^{2–5} For example, Doshi *et al.* reported a peak power density of 140 mW cm^{-2} at 500°C for a hydrogen-air fuel cell with an anode-supported $\text{Ce}_{0.8}\text{Gd}_{0.2}\text{O}_{1.9}$ electrolyte.² However, they also pointed out a reduction of Ce^{4+} to Ce^{3+} by hydrogen above 450°C, thus resulting in mixed oxide-ionic and electronic conduction. This leads to a reduction of the open-circuit voltage (OCV) and thus to an energy loss, which becomes more important as the operating temperature increases.

One effective approach to such a problem has been proposed by Eguchi and co-workers.^{8,9} A thin YSZ film was deposited at the fuel side of the electrolyte by radio-frequency (rf) sputtering. The YSZ-coated ceria-based electrolyte exhibited higher OCVs than an uncoated ceria-based electrolyte. Following their work, similar investigations and characterizations have been carried out by many research groups.^{10–13} However, this technique shows some major disadvantages: (i) delamination and cracking of the YSZ film; (ii) large polarization resistance when using the YSZ electrolyte; and (iii) high fabrication cost and small-scale fabrication. In this study, we report a more practical and effective method for suppressing the reduction of ceria by fuel gases, where a thin $\text{BaCe}_{1-x}\text{M}_x\text{O}_{3-\alpha}$ layer ($\text{M} =$ a dopant cation in the electrolyte used) is grown by a solid-state reaction of the electrolyte substrate and a thin BaO film deposited previously over the substrate surface at elevated temperatures. Experimental evidence for the superiority of the $\text{BaCe}_{1-x}\text{M}_x\text{O}_{3-\alpha}$ layer to the YSZ film is presented. Furthermore, an SOFC with the improved electrolyte exhibits excellent fuel-cell performances.

Experimental

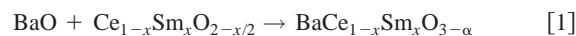
A thin $\text{BaCe}_{1-x}\text{Sm}_x\text{O}_{3-\alpha}$ layer was synthesized over the surface of a samaria-doped ceria (SDC, $\text{Ce}_{0.8}\text{Sm}_{0.2}\text{O}_{1.9}$) electrolyte as fol-

lows. A slurry of BaO was prepared by mixing the corresponding powders, ethyl cellulose, butyl carbitol, and terpineol in a planetary ball mill at 150 rpm for 4 h. The slurry was screen printed over one surface of the SDC pellet (diameter 13 mm; thickness 0.5 mm). The thickness of the BaO film was several decades of micrometers; however, this value does not reflect an exact thickness of BaO because of a large amount of organic binders in the film. After drying at 130°C, the pellet was heated between 900 and 1500°C for 10 h in air to proceed a solid-state reaction of BaO and SDC. Changes in the pellet surface after sintering were observed by X-ray diffraction (XRD) and scanning electron microscopy (SEM) techniques coupled to an energy dispersive X-ray (EDX) detector.

A 30 wt % SDC-containing NiO anode slurry (area 0.5 cm^2) was applied to the surface of the $\text{BaCe}_{1-x}\text{Sm}_x\text{O}_{3-\alpha}$ layer, followed by firing at 1400°C in air for 1 h. An $\text{Sm}_{0.5}\text{Sr}_{0.5}\text{CoO}_3$ cathode slurry (area 0.5 cm^2) was applied to the surface of the SDC pellet and then fired at 900°C in air for 4 h. The preparation and treatment of these electrodes were described in detail elsewhere.^{14,15} Two gas chambers were set up by placing the cell between two alumina tubes. Each chamber was sealed by melting a glass ring gasket at 950°C. Electrical collection in the cell was performed using an Au mesh for the anode and a Pt mesh for the cathode. The fuel chamber was supplied with wet hydrogen, which was saturated with H_2O vapor at room temperature, at 30 mL min^{-1} . The air chamber was statically exposed to atmospheric air. Fuel-cell performances were evaluated between 600 and 950°C. The current density-cell voltage curves and the impedance spectra of the cell were measured using a galvanostat and an impedance analyzer, respectively.

Results and Discussion

Figure 1 shows XRD patterns of the BaO-coated surface of the SDC electrolyte after sintering at different temperatures. Some unidentified peaks other than those assigned to SDC were present before sintering; probably, these peaks may be attributed to the organic binders used. Peaks assigned to the perovskite phase were observed by sintering the SDC electrolyte between 900 and 1500°C, which suggests that the following solid-state reaction began to proceed above 900°C



Another important point is the notion that the peak intensity for SDC was minimized at 1100°C and then enhanced above 1300°C. This may be explained by penetration of Ba^{2+} ion into the electrolyte bulk or diffusion of Ce^{4+} ion toward the top of the surface.

The microstructure of the $\text{BaCe}_{1-x}\text{Sm}_x\text{O}_{3-\alpha}$ layers shown above was characterized by SEM and EDX (Fig. 2). The SEM images

* Electrochemical Society Active Member.

^z E-mail: takashi.hibino@urban.env.nagoya-u.ac.jp

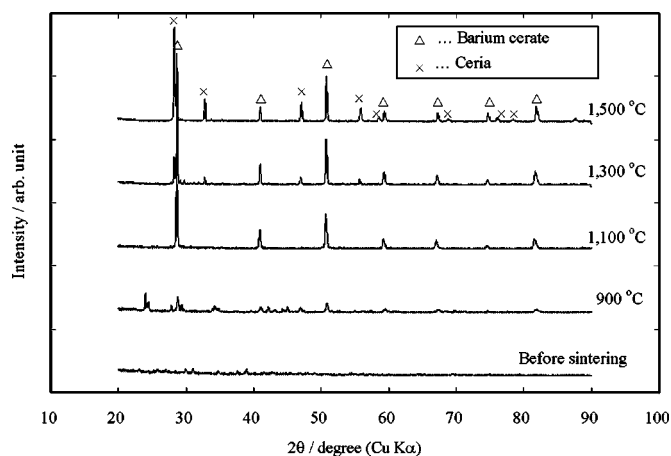


Figure 1. XRD patterns of BaO-coated surface of SDC electrolyte after sintering at different temperatures.

showed that although the $\text{BaCe}_{1-x}\text{Sm}_x\text{O}_{3-\alpha}$ layers grown at any temperature appeared to be well bonded to the electrolyte surface, the boundaries between the layer and the electrolyte gradually disappeared as the sintering temperature increased. As a result, the $\text{BaCe}_{1-x}\text{Sm}_x\text{O}_{3-\alpha}$ layer grown at 1500°C was the best united with the electrolyte substrate. As described later, such a continuous network led to good long-term stability of the layer. EDX mapping revealed that the thickness of the $\text{BaCe}_{1-x}\text{Sm}_x\text{O}_{3-\alpha}$ layer grown at 1500°C was about 12 μm . Furthermore, this layer included a Ce-rich phase few micrometers thick in the neighborhood of the external surface, which is consistent with the XRD results shown above.

BaCeO_3 thermodynamically reacts with CO_2 to form carbonates below 1200°C.¹⁶ We thus evaluated the chemical stability of the $\text{BaCe}_{1-x}\text{Sm}_x\text{O}_{3-\alpha}$ layers produced at different temperatures to CO_2 . From the XRD patterns of the $\text{BaCe}_{1-x}\text{Sm}_x\text{O}_{3-\alpha}$ layers after exposure to CO_2 at 950°C (Fig. 3), it follows that the layer did not react with CO_2 if sintered at 1500°C, below which the layer was decomposed into BaCO_3 and CeO_2 in the presence of CO_2 . After experiments, the surface of the former layer remained almost unchanged, whereas the surface of the latter layers was darkly colored. A possible explanation for this behavior is the notion that the Ce-rich phase localized in the vicinity of the external surface of the

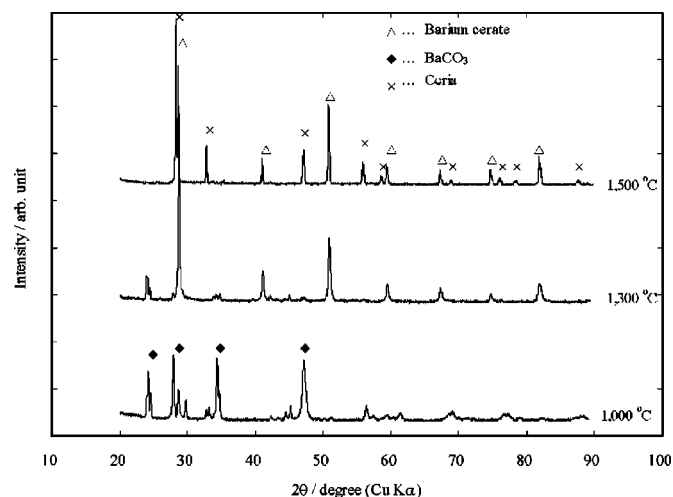


Figure 3. XRD patterns of $\text{BaCe}_{1-x}\text{Sm}_x\text{O}_{3-\alpha}$ layers after exposing to CO_2 . The three layers were grown by sintering at 1000, 1300, and 1500°C, respectively. CO_2 treatment was made by exposing the samples to a mixture of 50 vol % CO_2 and 50 vol % Ar at 950°C at a flow rate of 30 mL min^{-1} for 1 h.

$\text{BaCe}_{1-x}\text{Sm}_x\text{O}_{3-\alpha}$ layer acts as a protective layer against CO_2 . Taking into account this high tolerance to CO_2 together with the unification of the layer with the electrolyte substrate, we chose the SDC electrolyte growing the $\text{BaCe}_{1-x}\text{Sm}_x\text{O}_{3-\alpha}$ layer at 1500°C in subsequent experiments.

Performances of a hydrogen-air fuel cell were evaluated between 600 and 950°C. The OCVs generated from the cell are plotted against the operating temperature in Fig. 4, which also includes the data for two cells using the untreated SDC and $\text{BaCe}_{0.8}\text{Sm}_{0.2}\text{O}_{3-\alpha}$ electrolytes. While the OCVs of the cell with the untreated SDC electrolyte were much lower than the theoretical values, those of the cell with the treated SDC electrolyte were near those of the cell with the $\text{BaCe}_{0.8}\text{Sm}_{0.2}\text{O}_{3-\alpha}$ electrolyte, which is an almost purely ionic conductor in reducing atmospheres.¹⁷ This result indicates that the $\text{BaCe}_{1-x}\text{Sm}_x\text{O}_{3-\alpha}$ layer blocks off the electronic current successfully in the range of 600-950°C. The OCV of the cell was stable; no observable decrease in OCV was found for a period of at least 100 h. The strong junction between the layer and the electrolyte described above leads to high stability of the OCV.

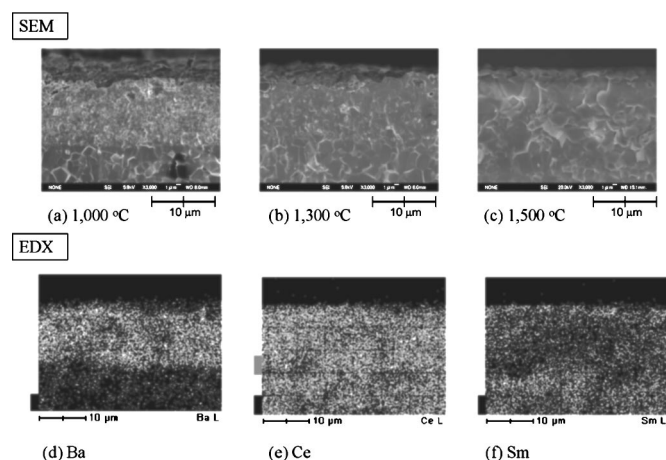


Figure 2. SEM and EDX observations of BaO-coated surface of SDC electrolyte after sintering at different temperatures. SEM images (a), (b), and (c) show the electrolyte surfaces after sintering at 1000, 1300, and 1500°C, respectively. The element mappings (d), (e), and (f) show the results for Ba, Ce, and Sm, respectively, of the electrolyte surface after sintering at 1500°C.

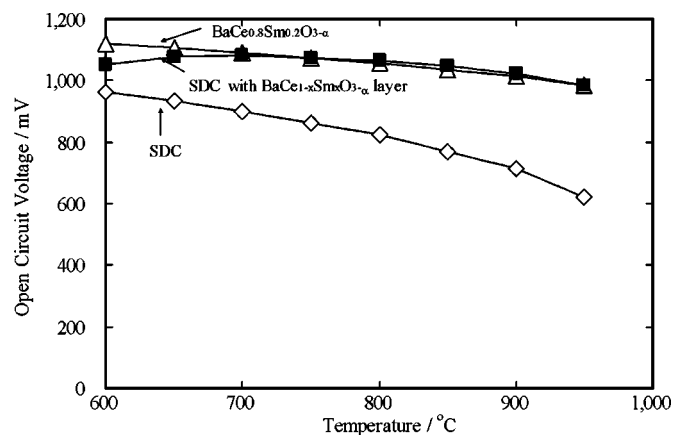


Figure 4. OCVs generated from three SOFCs as a function of operating temperature: Ni-30 wt % SDC[uncoated or coated SDC (0.5 mm thick) | $\text{Sm}_{0.5}\text{Sr}_{0.5}\text{CoO}_3$; Ni| $\text{BaCe}_{0.8}\text{Sm}_{0.2}\text{O}_{3-\alpha}$ (0.5 mm thick)|Pt]. The anode chamber was supplied with hydrogen, which was saturated with H_2O vapor at room temperature, at 30 mL min^{-1} . The cathode was statically exposed to atmospheric air.

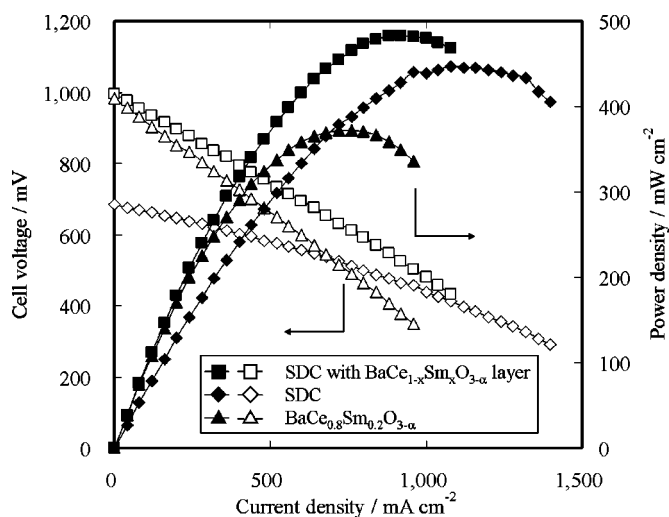


Figure 5. Discharge properties of three SOFCs at 950°C. The other experimental conditions are the same as those in Fig. 4.

The discharge properties of the above three cells at 950°C are shown in Fig. 5. Although current could be drawn from the three cells, the voltage drop during cell discharge was dependent upon the electrolyte materials used; the voltage drop was in the order of $\text{BaCe}_{0.8}\text{Sm}_{0.2}\text{O}_{3-\alpha} > \text{SDC with BaCe}_{1-x}\text{Sm}_x\text{O}_{3-\alpha} \text{ layer} > \text{SDC}$. The impedance spectra of the three cells further clarified this point; the order of the ohmic resistance was $\text{SDC} (0.18 \Omega \text{ cm}^2) < \text{SDC with BaCe}_{1-x}\text{Sm}_x\text{O}_{3-\alpha} \text{ layer} (0.24 \Omega \text{ cm}^2) < \text{BaCe}_{0.8}\text{Sm}_{0.2}\text{O}_{3-\alpha} (0.33 \Omega \text{ cm}^2)$; the order of the total polarization resistance was $\text{SDC} (0.02 \Omega \text{ cm}^2) < \text{SDC with BaCe}_{1-x}\text{Sm}_x\text{O}_{3-\alpha} \text{ layer} (0.08 \Omega \text{ cm}^2) < \text{BaCe}_{0.8}\text{Sm}_{0.2}\text{O}_{3-\alpha} (0.07 \Omega \text{ cm}^2)$. Therefore, the smallest voltage drop for the cell with the untreated SDC electrolyte was attributable to both the smallest ohmic and polarization resistances. Nonetheless, it must be emphasized that the extremely small polarization resistance of the cell with the untreated SDC electrolyte was due to an increase of the reaction zone at the three-phase boundaries by electronic conduction in the electrolyte.¹⁸ It is reasonable to presume that if the SDC electrolyte is not entirely reduced by hydrogen, the polarization resistance is near that using the SDC electrolyte with a $\text{BaCe}_{1-x}\text{Sm}_x\text{O}_{3-\alpha}$ layer. Figure 5 also shows that the peak power density of the cell using the SDC electrolyte with the $\text{BaCe}_{1-x}\text{Sm}_x\text{O}_{3-\alpha}$ layer reached 482 mW cm^{-2} , which is the highest among the three cells. More important, the power density of the cell using this electrolyte was 416 mW cm^{-2} at a cell voltage of 0.7 V, while the cell using the untreated SDC electrolyte no longer functioned as a fuel cell.

Protons, besides oxide ions, serve as the charge carriers in BaCeO_3 -based electrolytes.^{17,19} We attempted to determine whether

proton conduction occurs in the $\text{BaCe}_{1-x}\text{Sm}_x\text{O}_{3-\alpha}$ layer. An H/D isotope effect would give useful information about this point because of the large 1:2 mass ratio of H^+ and D^+ .²⁰⁻²³ Impedance measurements showed that there was no difference in ohmic resistance of the cell between H_2 and D_2 fuels, which provides primary evidence that protons do not contribute to the ionic conductivity in the $\text{BaCe}_{1-x}\text{Sm}_x\text{O}_{3-\alpha}$ layer. It seems likely that the SDC electrolyte intercepts proton migration from the anode to the cathode.

We expect that our method may be applied to other ceria-based electrolytes. Similar results were obtained for a gadolinia-doped ceria (GDC; $\text{Ce}_{0.9}\text{Gd}_{0.1}\text{O}_{1.95}$; 0.5 mm thick). However, the SOFC showed a peak power density of 408 mW cm^{-2} , which is lower than the value shown in Fig. 5, although it generated an OCV almost equal to the value shown in Fig. 5. It has been reported that the ionic conductivity of $\text{BaCe}_{1-x}\text{Gd}_x\text{O}_{3-\alpha}$ materials increases with the Gd content.¹⁹ Therefore, we assumed that the smaller Gd^{3+} amount of 10 mol % in the GDC electrolyte resulted in a lower ionic conductivity of the $\text{BaCe}_{1-x}\text{Gd}_x\text{O}_{3-\alpha}$ layer produced over the surface, which enhanced the ohmic resistance of the cell. This assumption suggests that the fuel-cell performances would be further improved by using GDC electrolytes with higher Gd^{3+} content.

The National Institute of Advanced Industrial Science and Technology assisted in meeting the publication costs of this article.

References

1. B. C. H. Steele and A. Heinzel, *Nature (London)*, **414**, 345 (2001).
2. R. Doshi, R. Von L. Richards, J. D. Carter, X. Wang, and M. Krumpelt, *J. Electrochem. Soc.*, **146**, 1273 (1999).
3. B. C. H. Steele, *Solid State Ionics*, **129**, 95 (2000).
4. M. Mogensen, N. M. Sammes, and G. A. Tompsett, *Solid State Ionics*, **129**, 63 (2000).
5. H. L. Tuller, *Solid State Ionics*, **131**, 143 (2000).
6. T. Ishihara, H. Matsuda, and Y. Takita, *J. Am. Chem. Soc.*, **116**, 3801 (1994).
7. P. Lacombe, F. Goutenoire, O. Bohnke, R. Retoux, and Y. Laligant, *Nature (London)*, **404**, 856 (2000).
8. T. Inoue, T. Setoguchi, K. Eguchi, and H. Arai, *Solid State Ionics*, **35**, 285 (1989).
9. K. Eguchi, T. Setoguchi, T. Inoue, and H. Arai, *Solid State Ionics*, **52**, 165 (1992).
10. A. V. Virkar, *J. Electrochem. Soc.*, **138**, 1481 (1991).
11. F. M. B. Marques and L. M. Navarro, *Solid State Ionics*, **90**, 183 (1996).
12. S. Hamakawa, T. Hayakawa, T. Tsunoda, K. Suzuki, K. Murata, and K. Takehira, *Electrochem. Solid-State Lett.*, **1**, 220 (1998).
13. S. H. Chan, X. J. Chen, and K. A. Khor, *Solid State Ionics*, **158**, 29 (2003).
14. T. Hibino, A. Hashimoto, T. Inoue, J. Tokuno, S. Yoshida, and M. Sano, *Science*, **288**, 2031 (2000).
15. T. Hibino, A. Hashimoto, M. Yano, M. Suzuki, S. Yoshida, and M. Sano, *J. Electrochem. Soc.*, **149**, A133 (2002).
16. M. J. Scholten, J. Schoonman, J. C. van Miltenburg, and H. A. Oonk, *Solid State Ionics*, **61**, 83 (1993).
17. H. Iwahara, T. Yajima, T. Hibino, and H. Ushida, *J. Electrochem. Soc.*, **140**, 1687 (1993).
18. T. Takahashi, H. Iwahara, and I. Ito, *Denki Kagaku oyobi Kogyo Butsuri Kagaku*, **38**, 509 (1970).
19. N. Bonanos, K. S. Knight, and B. Ellis, *Solid State Ionics*, **79**, 161 (1995).
20. T. Norby, *Solid State Ionics*, **40-41**, 857 (1990).
21. R. C. T. Slade and N. Singh, *J. Mater. Chem.*, **1**, 441 (1991).
22. J. Liu and A. S. Nowick, *Solid State Ionics*, **50**, 131 (1992).
23. T. Hibino and H. Iwahara, *J. Electrochem. Soc.*, **141**, L125 (1994).